Effective Optimization of the Control System for the Cement Raw Meal Mixing Process: II. Optimizing Robust PID Controllers Using Real Process Simulators

DIMITRIS TSAMATSOULIS
Halyps Building Materials S.A., Italcementi Group
17th Klm Nat. Rd. Athens – Korinth
GREECE
d.tsamatsoulis@halyps.gr http://www.halyps.gr

Abstract: - The present study is aiming to develop a simulator of the mixing process in production installations of raw meal comprising all the main characteristics of the process and raw materials. The system is described by a TITO process regarding the adjustment of the two main quality indicators of the raw meal and regulated via PID controllers. The M - Constrained Integral Gain Optimization (MIGO) method is used to tune the controller parameters. Based on actual industrial data the simulator is implemented to determine the optimum PID parameters according to the subsequent criteria: (a) specified robustness constraint and (b) minimum variance of the raw mix chemical modules in raw mill outlet and kiln feed. The simulator offers the possibility to analyze the effect of the process parameters on the raw meal homogeneity. Other digital PID implementations except the one utilized or other control laws can be investigated as well.

Key-Words: - Dynamics**,** Raw meal, Quality, Mill, Simulation, Uncertainty, PID, Robustness

1 Introduction

Historically, advanced process control efforts in cement products quality have focused on raw meal homogeneity as it is the main factor influencing the clinker activity [1]. Primarily the control and regulation is performed in the raw mill outlet.

In Figure 1 a typical flow chart of raw meal production is shown, including three raw materials feeders.

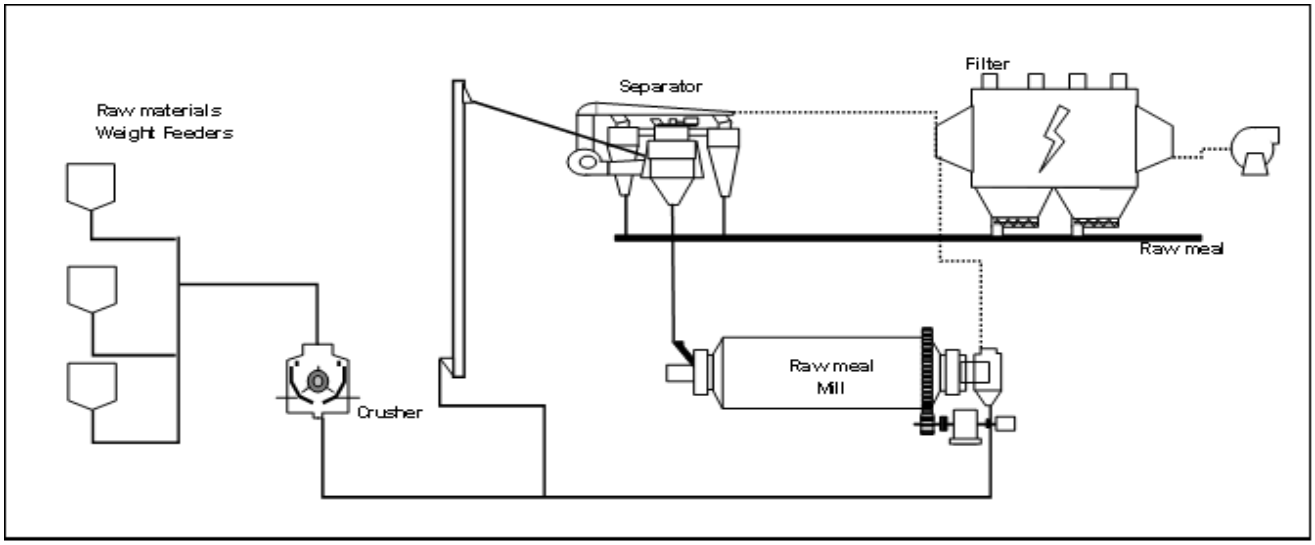

Figure 1. Flow chart of raw meal production

In the demonstrated closed circuit process, the crusher and mill outlets go through the recycle elevator to a dynamic separator. The fine exit stream of the separator is the main part of the final product. The coarse separator return, is directed to the mill, where is ground again. The material in the mill and classifier are dried and de-dusted by hot gas flow. This is a standard flow sheet encountered to the most of the raw meal dry grinding processes performed in ball mills.

Because the raw mix composition affects clinker reactivity, clinker formation conditions, kiln thermal consumption and bricks lining, it is of high value to keep the raw meal quality variance in the lowest

feasible level. Due to complexity and significance of the process, various automated systems are available for sampling and analyzing the raw mix as well as for adjustment of the mill feeders according to the raw meal chemical modules in the mill (RM) outlet. The regulation is mainly obtained via PID and adaptive controllers [2, 3]. As clearly Kural et al. [3] declare, the disturbances coming from the variations in the chemical compositions of the raw materials from long-term average compositions cause the changes of the system's parameters. Tsamatsoulis [4] built a reliable model of the dynamics among the chemical modules in the outlet of a raw meal grinding system and the proportion of the raw materials. This model was utilized in [5] to feed with inputs, techniques of advanced automatic control, in order a robust PID controller to be achieved, able to reject disturbances affecting the raw meal quality. The conclusion of these efforts is that to design a robust raw meal controller, furthermore satisfying a given sensitivity constraint [6, 7], an efficient modeling of the process is obligatory.

Adaptive controllers of varying degrees of complexity have been also elaborated [8, 9]. However in the industrial process control more than 95% of the control loops are of PID type [10] and moreover only a small portion of them operate properly [11]. Tsamatsoulis [12] tuned a classical PID controller among chemical modules in the RM output and raw materials proportion in the mill feed, using as optimization criterion the minimum variance of these modules in the kiln feed. He concluded that the application of stability criteria is necessary. He also proved that the variance of the kiln feed composition not only depends on the raw materials variations and the mixing capacity of the silos but also it is strongly related with the effectiveness of the regulating action. A widely applied methodology to derive robust and operative controllers is the loop shaping method [13, 14, 15, 16, 17]. An extremely efficient loop shaping technique to tune PID controllers is called MIGO (M- constrained integral gain optimization) [10, 18, 19]. The design approach is to maximize integral gain fulfilling a constraint on the maximum sensitivity.

The aim of the present analysis is to try to optimize robust PID controllers regulating the raw meal quality, previously parameterized with the MIGO methodology. To reach this challenging target extensive simulations of the actual raw meal mixing process during grinding and storage are built. The developed simulators comprise the large majority of the process parameters and their uncertainty as well. As to the dynamical data of the mill and silos, the results of [4] are utilized, determined from the processing of long term quality data of Halyps cement plant. Actual raw materials compositions are also examined, involving their variance. The sets of PID computed for the same mill installation according to the MIGO technique [5], are used as inputs as well.

2 Process Model

2.1 Proportioning Modules Definition

For the main oxides contained in the cement semifinal and final products, the following abbreviations are commonly used in the cement industry: C=CaO, S=SiO_2, A=Al_2O_3, F=Fe_2O_3. Three proportioning modules are used to indicate the quality of the raw meal and clinker. [1]:

$$Lime\ Saturation\ Factor$$
$$LSF = \frac{100 \cdot C}{2.8 \cdot S + 1.18 \cdot A + 0.65 \cdot F} \quad (1)$$

$$Silica\ Modulus\ \ SM = \frac{S}{A + F} \quad (2)$$

$$Alumina\ Modulus\ \ AM = \frac{A}{F} \quad (3)$$

The regulation of some or all of the indicators (1) to (3) contributes drastically to the achievement of a stable clinker quality.

2.2 Block Diagram and Transfer Functions

The block diagram shown in Figure 2 and the respective transfer functions are presented and investigated in [5] and repeated here for elucidation reasons.

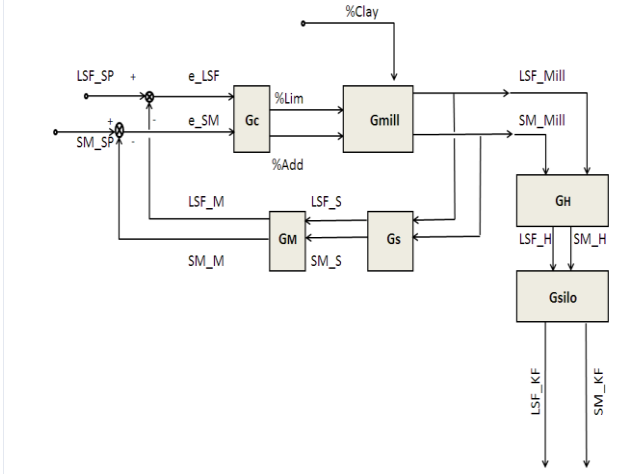

Figure 2. Block diagram of the grinding and blending process.

Each block represents one or more transfer functions: G_c symbolizes the transfer function of the controller. With G_{mill}, the RM transfer function is indicated, containing three separate functions. The raw meal sampling in the RM outlet is performed via a sampling device, accumulating an average sample during the sampling period. The integrating action of the sampler is denoted by the function G_s. The delay caused by the sample preparation and analysis is shown by the function G_M. The raw meal is homogenized in overflow silo with transfer function G_H. Then the raw meal before to enter to the kiln is stocked to a storage silo with transfer function G_{silo}.

%Lim, %Add, %Clay = the percentages of the limestone, additive and clay in the three weight feeders. LSF_{Mill}, SM_{Mill} = the spot values of LSF and SM in the RM outlet, while LSF_S, SM_S, LSF_M, SM_M = the modules of the average sample and the measured one. Finally LSF_H, SM_H, LSF_{KF}, SM_{KF} = the corresponding modules in the homo silo outlet and in the kiln feed. LSF and SM set points are indicated by LSF_{SP} and SM_{SP} respectively, while e_LSF and e_SM stand for the error between set point and respective measured module.

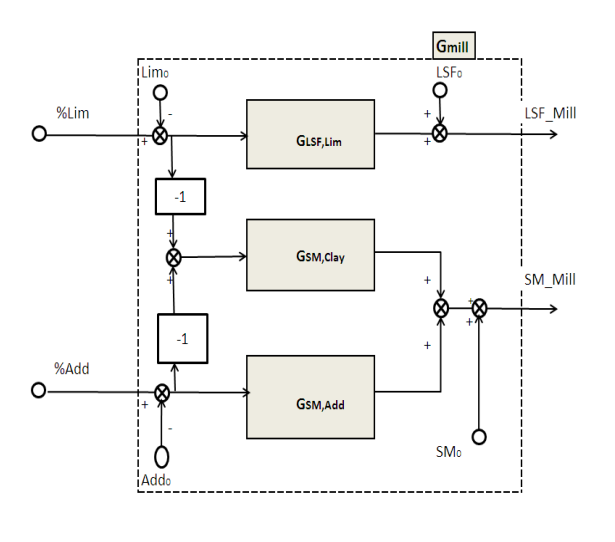

Figure 3. Transfer functions of the RM block.

The block of the raw meal mixing in the RM is analyzed in more detail in Figure 3.The functions between the modules and the respecting percentages of the raw materials are indicated by $G_{LSF,Lim}$, $G_{SM,Clay}$, $G_{SM,Add}$.

The G_M function, representing a pure delay, is described by equation (4):

$$G_M = e^{-tM \cdot s} \tag{4}$$

The delay t_M is composed by the time intervals of sample transferring, preparation, analysis and computation of the new settings of the three feeders and finally transfers of those ones to the weight scales. The function G_s is defined by the formula (5):

$$G_s = \frac{1}{T_s \cdot s}(1 - e^{-Ts \cdot s}) \tag{5}$$

Based on previous results [4, 5] a second order with time delay (SOTD) model is chosen for each of the functions $G_{LSF,Lim}$, $G_{SM,Clay}$, $G_{SM,Add}$ described by the equation (6):

$$G_x = \frac{k_{g,x}}{\left(1 + T_{0,x} \cdot s\right)^2} \cdot e^{-td,x \cdot s} \tag{6}$$

Where x = Lim, Clay or Add. The constant k_g, T_0, t_d symbolize the gain, the time constant and the time delay respectively. In the time domain the functions (6) are expressed by the equations (7) and (8):

$$LSF - LSF_0 = k_{g,Lim} \cdot \left(1 - \exp\left(-\frac{t - t_{d,Lim}}{T_{0,Lim}}\right) - \frac{t - t_{d,Lim}}{T_{0,Lim}} \cdot \exp\left(-\frac{t - t_{d,Lim}}{T_{0,Lim}}\right)\right) \cdot (Lim - Lim_0) \tag{7}$$

The parameters Lim_0 and LSF_0 symbolize the steady state values of the input and output variables. $Clay_0$, Add_0 and SM_0 correspond also to steady state values. $Clay_0$ is not an independent variable but given from the difference 100- Lim_0-Add_0. The LSF and SM variables of the functions (7), (8) represent the modules in RM outlet corresponding also to the homo inlet $LSF_{H,In}$, $SM_{H,In}$.

$$SM - SM_0 = k_{g,Clay} \cdot \left(1 - \exp\left(-\frac{t - t_{d,Clay}}{T_{0,Clay}}\right) - \frac{t - t_{d,Clay}}{T_{0,Clay}} \cdot \exp\left(-\frac{t - t_{d,Clay}}{T_{0,Clay}}\right)\right) \cdot (Clay - Clay_0) + k_{g,Add} \cdot \left(1 - \exp\left(-\frac{t - t_{d,Add}}{T_{0,Add}}\right) - \frac{t - t_{d,Add}}{T_{0,Add}} \cdot \exp\left(-\frac{t - t_{d,Add}}{T_{0,Add}}\right)\right) \cdot (Add_0 - Add) \tag{8}$$

To avoid elevated degrees of freedom the following equalities are considered:

$$T_{0,Clay} = T_{0,Add} \quad t_{d,Clay} = t_{d,Add} \tag{9}$$

The homo and stock silo transfer functions are given by the first order equations (10) and (11) respectively:

$$G_H = \frac{y_H}{y_{H,In}} = \frac{1}{1 + T_H \cdot s} \tag{10}$$

$$G_{Silo} = \frac{y_{KF}}{y_H} = \frac{1}{1 + T_{Silo} \cdot s} \tag{11}$$

Where y_H=LSF_H or SM_H, $y_{H,In}$=$LSF_{H,In}$ or $SM_{H,In}$, y_{KF}=LSF_{KF} or SM_{KF}. T_H and T_{Silo} represent the homo and stock silo first order time constants.

The model parameters are evaluated in [5] using hourly data of feeders' percentages and proportioning modules of the first seven months of 2010. The procedure to estimate the mean parameters of the raw mill dynamics and their uncertainty as well is analytically described in [4]. As concerns the RM dynamics, the results are depicted in Table 1.

Table 1. Average and standard deviation of the model parameters

	Average	Standard Dev.
$K_{g,Lim}$	2.96	0.82
$T_{0,Lim}$(h)	0.19	0.15
$t_{d,Lim}$(h)	0.41	0.13
$K_{g,Clay}$	0.036	0.030
$K_{g,Add}$	0.437	0.291
$T_{0,Add}$(h)	0.33	0.18
$t_{d,Add}$(h)	0.33	0.18

The time constants of the homo and stock silos transfer functions are found using the AM module silos' input and output [5]. As the homo silo operates with overflow, it is always considered to be full. As to the stock silo, the empty meters during the operation are also taken into account. The processing of one full year data provides the following results:

$$T_H = 3.0 \pm 0.6\ h$$

$$T_{Silo} = 16.3 \cdot H_E^{-0.6} \pm 1.3\ h \tag{12}$$

Where H_E= the empty meters of the stock silo. To notice that each meter of the stock contains 330 tons of raw meal.

3 Simulator Design

3.1 Simulator's Description

All the main characteristics and steps of the raw meal production process are taken into consideration during the procedure of simulator preparation. The simulation starts from the materials' input to the RM and ends when the raw meal is fed to the kiln.

Limestone and clay are fed to the mill via two silos: the first silo contains limestone while the second one a mixture of limestone and clay with volume ratio limestone/clay=0.5. The bulk densities of the two materials are considered the same. The third silo contains the corrective material composed from iron oxide and bauxite with a fixed volume ratio. The bulk density of the iron oxide is the double of the bauxite's respective density. For the same time period that the RM dynamics is determined, the raw materials analysis is considered. From all the spot samples of limestone and clay, the average values and standard deviations of the main oxides and moistures are found. To calculate the standard deviations, the outliers are excluded by applying ISO 8258:1991. Thus, data represent the routine raw materials fed to the RM and because of the large number of analysis, the data distribution is normal.

Table 2. Raw materials analysis

	Limestone		Clay	
Oxide	Aver.	Std. Dev.	Aver.	Std. Dev.
SiO_2	1.25	0.35	43.32	4.80
Al_2O_3	0.50	0.12	7.52	1.08
Fe_2O_3	0.29	0.07	3.98	0.51
CaO	54.18	0.67	20.79	3.82
%Moist.	3.4	1.2	10.2	1.7
N	31		112	
LSF	1266		15.7	
	Average		Std. Dev.	
Lim./ Clay	0.5		0.1	
Oxide	Iron Oxide		Bauxite	
SiO_2	1.0		4.1	
Al_2O_3	0.5		38.9	
Fe_2O_3	95.0		8.5	
CaO	1.0		20.6	
Baux /Iron	3.0			

As to the corrective compounds, due to their low dosage, their analysis is thought as stable. The magnitude of the standard deviation constitutes the uncertainty's measure. An uncertainty is also supposed to the limestone/clay ratio fed to the RM from the second silo. These data are presented in Table 2. As to the time constants and delay times of the RM dynamical model, the values shown in Table 1 constitute the simulator inputs. All the times are expressed in hours.

Afterwards the simulator proceeds in the following way: A time period, T_{tot}, of raw mill operation is decided, not necessarily continuous. The limestone composition is supposed constant for a time interval, not exactly determined, but considered to be between $T_{Min,Lim}$ and $T_{Max,Lim}$. Then by utilizing a random generator, a random number, x, between 0 and 1 is selected. To find the interval of constant limestone the formula (13) is applied.

$$T_{Const,Lim} = Int\left(\left(T_{Max,Lim} - T_{Min,Lim} + 1\right)\cdot x + T_{Min,Lim}\right) \quad (13)$$

Exactly the same procedure is followed to find a time interval of RM operation with constant clay composition, $T_{Const,Clay}$. The next step is to determine a constant composition for each raw material fed to the mill during $T_{Const,Lim}$ or $T_{Const,Clay}$ i.e. to determine oxides' analysis belonging to the range shown in Table 2: As previously a random number, x, belonging to the interval [0, 1] is chosen. Then for each raw material and oxide the inverse of the normal distribution is applied, with probability x, and the oxide percentage is found by the formula (14):

$$\%Oxide = NormInv(x, Ox_{Aver}, Ox_{StdDev}) \quad (14)$$

The same steps and equations (13), (14) are employed to define a period $T_{Const,Dyn}$ of constant RM dynamics, time constants and delay times for both LSF and SM dynamics, considering the dynamical data of Table 1. Therefore the period T_{tot} is partitioned in consecutive time intervals of constant limestone and clay feeding, $T_{Const,Lim}$ and $T_{Const,Clay}$ and stable RM dynamics, $T_{Const,Dyn}$. Equation (14) is also utilized to estimate the moistures of the raw materials, during the constant compositions' interval.

In the current level of development the simulator can regulate two chemical modules, LSF and SM. Consequently the respective target LSF_T and SM_T are defined. The sampling period T_s and measurement delay, T_M are also identified.

As shown in Figure 1, the filter dust is mixed with the RM product and both are directed to the homo silo. Therefore the dust's chemical composition constitutes simulator's input. Actual long term data are processed and the mean values and standard deviations of the oxides are determined. Then equation (14) is activated for each sampling interval. The mill dry production, the kiln feed flow rate and the filter dust flow rate constitute also critical inputs. Their balance derives the filling degree of the stock silo. An initial filling level is supposed expressed in empty meters. A minimum and a maximum level are introduced to the software and then by the application of equation (13), applied for height instead of time, the initial empty meters are found.

The regular operation case is to have a total flow rate feeding the homo silo higher than the kiln feed flow rate. Consequently raw mill shall stop when the empty meters of the stock silo arrive to a predefined minimum level H_{Min} and RM starts again to grind when the empty meters reach a maximum level H_{Max}. These levels are introduced to the simulator as initial data as well as the quantity of raw meal per meter of the storage silo. Initial homo and stock silos' chemical compositions are also introduced and the initial settings of the weight feeders as well. These initial conditions are usually selected near to the long term average or to the targets. As to the homo and storage silos dynamics, equations (12) are utilized. To cope with the uncertainties of the time constants, equation (14) is used for a more time.

LSF and SM modules are regulated using two independent PID controllers. Thus the TITO process is simplified to two SISO processes. The controllers are described by equation (15) in Laplace form:

$$\frac{u}{e} = k_p + \frac{k_i}{s} + k_d s \quad (15)$$

The variables k_p, k_i, k_d represent the proportional, integral and differential gains of the controller. The other variables have the following meaning: e = LSF_{SP}-LSF_M or SM_{SP}-SM_M, u = %Lim or %Add, (k_p,k_i,k_d) = (k_{pLSF},k_{iLSF},k_{dLSF}) or (k_{pSM},k_{iSM},k_{dSM}).This equation is expressed by equation (16) in discrete time domain, where as time interval, the sampling period is considered.

$$u_n = u_{n-1} + k_p\cdot(e_n - e_{n-1}) + T_s\cdot k_i\cdot e_n + k_d\cdot\frac{1}{T_s}\cdot(e_n + e_{n-2} - 2\cdot e_{n-1}) \quad (16)$$

The integral and differential times T_i and T_d are connected with the respective gains by equation (17).

$$k_i = {k_p}/{T_i} \ , \ k_d = k_p \cdot T_d \qquad (17)$$

The PID sets for the two controllers are selected among the computed ones in [5] for the same RM circuit. As robustness criterion in this previous analysis the Maximum Sensitivity was considered provided by equation (18):

$$M_s = Max(|S(i\omega)|) \qquad (18)$$

The sensitivity, S, is expressed by equation (19) as function of the process transfer function G_p, consisting of mixing in the mill, sampling and measuring transfer functions and the controller respective function G_c as well.

$$S = \frac{1}{1 + G_C G_p} \qquad (19)$$

As mentioned in [5] one of the main advantages of the M-constrained Integral Optimization Technique is that the robustness constraint is implied. In this way for each predetermined M_s, a full group of (k_p, k_i, k_d) parameters ranging from k_d=0 to a maximum value fulfilling the M_S constraint are computed. The k_p, k_i values as function of k_d and M_s for the two controllers are shown in Figures 4 to 7.

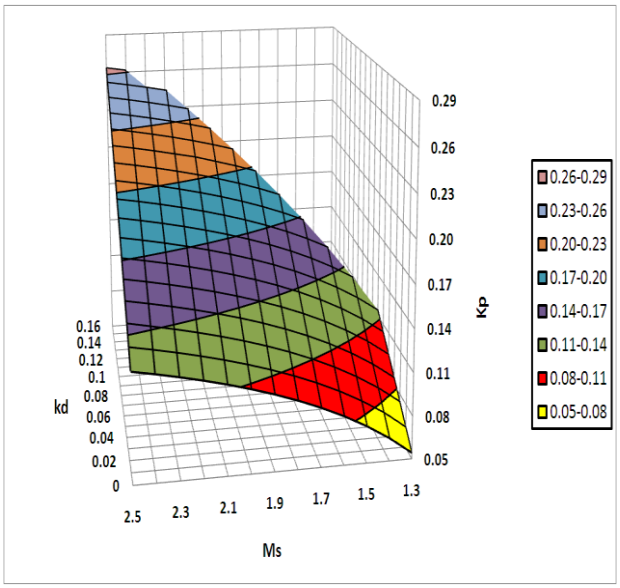

Figure 4. LSF controller. K_p as function of k_d, M_s.

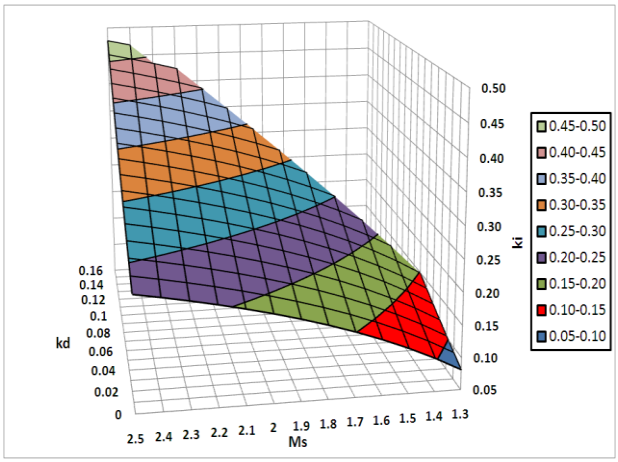

Figure 5. LSF controller. K_i as function of k_d, M_s.

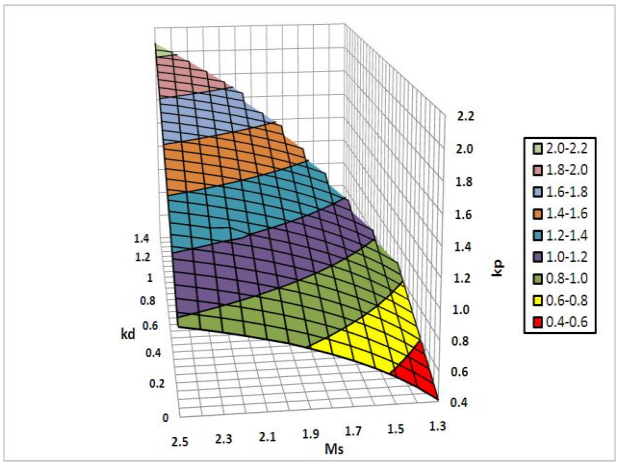

Figure 6. SM controller. K_p as function of k_d, M_s.

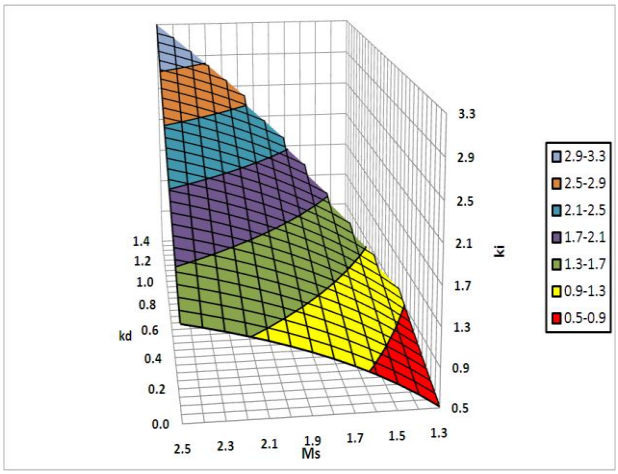

Figure 7. SM controller. K_i as function of k_d, M_s.

3.2 Operation of the Simulator

Afterwards the import of all data, the raw meal quality regulator runs as following:

(1) RM starts to run with the predefined settings of the weight feeders feeding the homo silo

(2) Te first average sample is taken after a T_s period and the composition is computed.

(3) Feedback is performed and both controllers provide the new settings to the feeders.
(4) In time interval T_s the average and spot analysis of the raw meal and the respective two modules are computed.
(5) The introduced raw meal to the homo silo is mixed with the existing one providing the material in homo outlet. To simplify the calculations, the material introduced to this silo is represented by the average analysis over the sampling period.
(6) The homo silo outlet constitutes the entry in the storage silo. There it is mixed with the active material's volume producing the raw meal feeding the kiln. Each T_s time interval the spot analysis of this raw meal is calculated.
(7) The simulator is checking after each sampling whether the empty volume of the stock silo, H_E, is lower than minimal permissible, H_{Min}
(8) If $H_E \leq H_{Min}$, RM stops and homo silo is fed only with the filter dust. Simultaneously the software is checking each T_s if $H_E \geq H_{Max}$.
(9) When the above occurs, RM starts again to operate and the software compares continuously H_E with H_{Min}. Otherwise RM remains stopped until the condition $H_E \geq H_{Max}$ would be fulfilled.
(10) During the time that material is supplied to the kiln all computations referred in steps (1) to (9) are permanently performed till the operating time of the mill becomes equal to T_{tot}.
(11) During the operation, all the chemical modules results in the different points of the circuit are saved.
(12) Afterwards their mean values and standard deviations are calculated. The total number the modules pass from the respective target – number of cuts – is also determined as it constitutes a significant quality indicator concerning the mixing performed in the homo silo.
(13) Due to fact that the initial data are generated randomly with respect of some specified limits, for the same initial settings the simulator performs a defined number of iterations. Then the average results of all the runs are computed. In this way some undesirable noise can be avoided.

An example of simulator application is shown in Figures 8 to 10. The following PID coefficients are utilized for M_s=1.5: (k_{pLSF}, k_{iLSF}, k_{dLSF}) = (0.152, 0.219, 0.08), (k_{pSM}, k_{iSM}, k_{dSM}) = (0.93, 1.15, 0.4). The simulation is applied for 240 hours of RM operation. In Figures 8 and 9 the LSF and SM in RM outlet are depicted. In the same Figures the settings of feeders are shown according to the controllers hourly actions. The LSF in RM outlet, homo outlet and kiln feed are demonstrated in Figure 10, where the mixing action of homo and stock silos clearly appears. The indicated hours correspond to kiln operation, including the hours where the mill does not function and homo silo is fed only with filter dust.

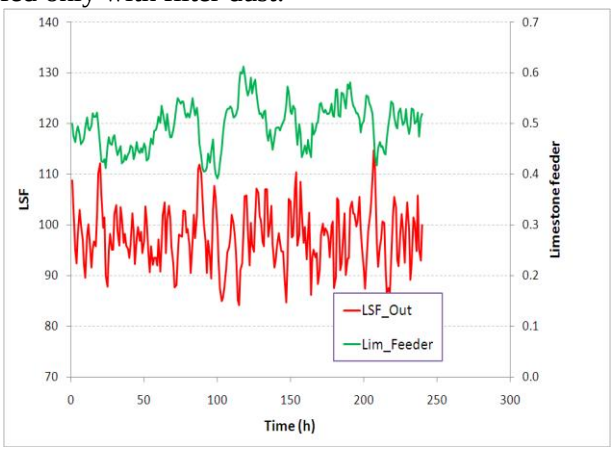

Figure 8. LSF in RM outlet and limestone feeder settings

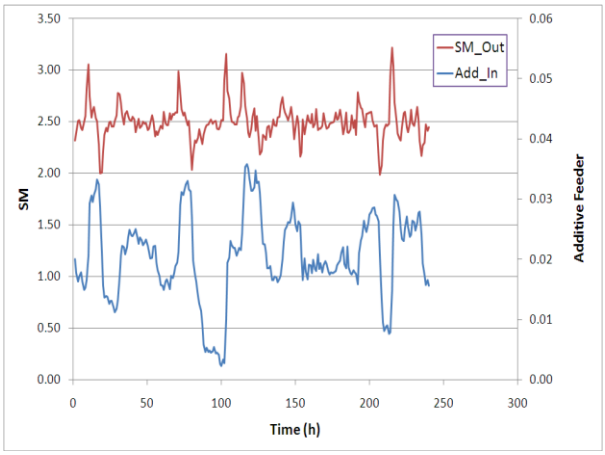

Figure 9. SM in RM outlet and limestone feeder settings.

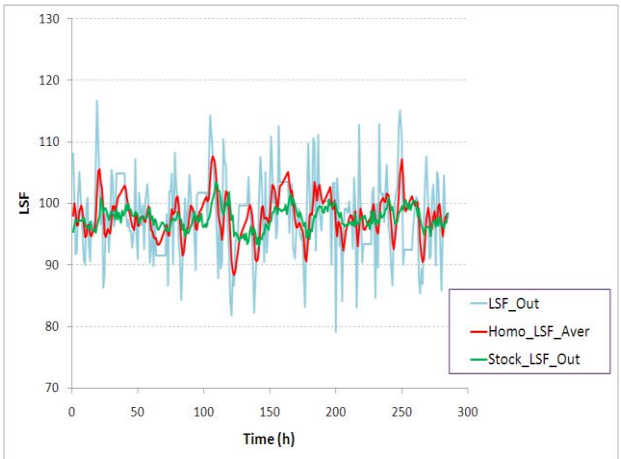

Figure 10. LSF in RM and homo outlet and kiln feed.

4 Implementation of the Simulator

4.1 Initial Simulations

Before the full implementation of the simulator, some initial simpler simulations are attempted, in order to be examined the characteristics of the loop. The (k_p, k_i, k_d) sets referred in section 3.1 are used.The set point tracking and the rejection of load disturbances are firstly investigated.

As a rule the chemical modules set points do not change frequently in raw meal milling systems. What habitually happens is the fact that during the RM start up, feeders' set point does not provide the module target, even if the raw materials composition is extremely stable. Thus a transient period appears, where the settling time and overshoot depends on the controller action. This situation is simulated in the following manner. The LSF target is put equal to 97.6. All the simulator parameters are considered that they have negligible variance and limestone feeder is initially located in a position deriving LSF_{In}=78.8, around 20 points less than the target. A continuous 64 hours RM operation is considered, by equating the RM productivity and kiln feed flow rate. As settling time it is defined the time where the mill outlet LSF remains constantly near to LSF_T in a region ±2% of the difference LSF_T-LSF_0. The overshoot is provided by the formula (20):

$$Overshoot = \left(\frac{LSF_{Max} - LSF_T}{LSF_T - LSF_0} - 1\right) \cdot 100 \qquad (20)$$

The simulation is applied for all the PID sets presented in Figures 4, 5. The settling time and overshoot results as function of M_s and k_d are presented in Figures 11, 12.

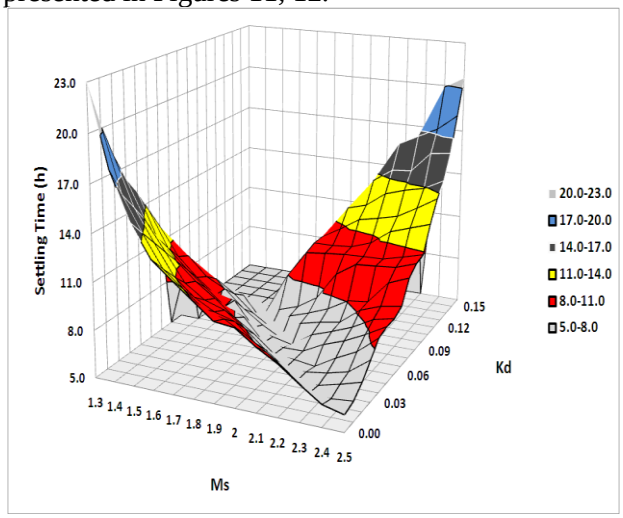

Figure 11. Set point tracking settling time as function of k_d, M_s.

The minimum settling time is found for M_s, k_d located in the diagonal of the [M_s, k_d] surface: As M_s augments, k_d shall be decreased to provide a settling time belonging to the region of minimum. The overshoot remains less than 1% for $M_s \leq 1.6$, for all the k_d range. Then, as M_s increases the k_d interval providing overshoot ≤ 1% becomes narrower.

The closed circuit response to a load disturbance has been treated as follows:

(a) The constraint of constant raw materials composition is relaxed and the raw materials compositions is computed according to section 3.1

(b) A 30 hours period is chosen as constant raw materials composition interval. Therefore the raw materials are kept constant for 30 hours and then their composition is altered for the next 30 hours. The above constitutes the load disturbance. A total running time of 60 hours is selected.

(c) All the other parameters are kept stable.

(d) After the initial period of 30 hours the load disturbance appears. To evaluate the controller performance for the various sets of (k_p, k_i, k_d), the maximum error from LSF_T and the settling time are determined. The latter in this case is defined as the time where the LSF in the mill outlet remains constantly near to LSF_T ± 0.2. The results are shown in Figure 13, 14.

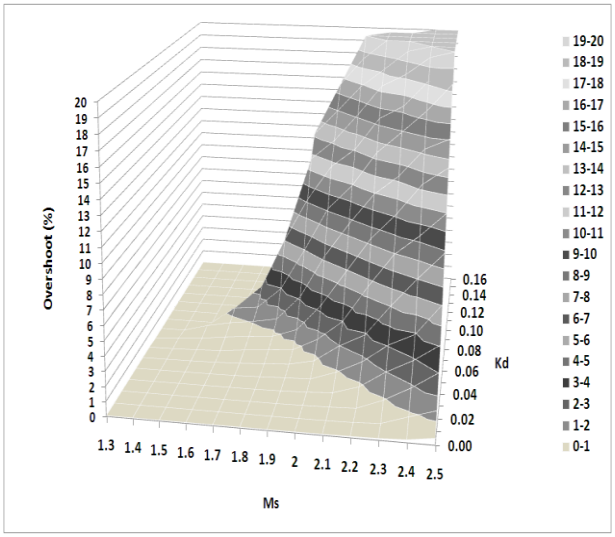

Figure 12. Set point tracking overshoot as function of k_d, M_s.

The impact of M_s and k_d onto the settling time after a load disturbance is exactly the same as in the set point tracking case. The maximum error gradually decreases as M_s and k_d are rising.

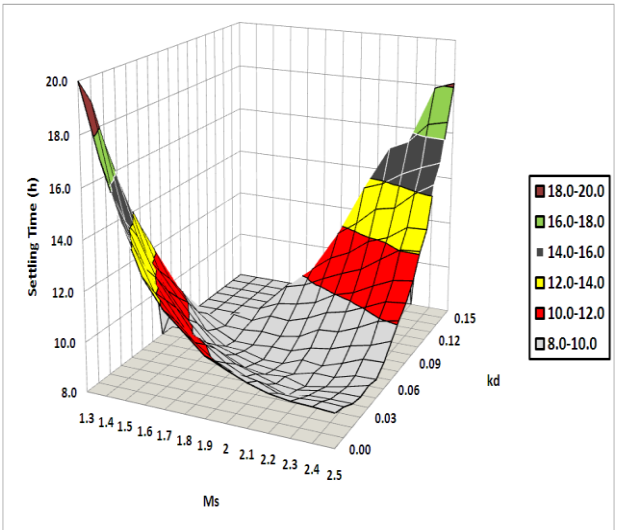

Figure 13. Load disturbance. Settling time as function of k_d, M_s.

To investigate deeper the achieved results, Figures 11 to 14 are combined in order to determine a region where: (a) Set point tracking settling time and overshoot are minimal. (b) Load disturbance settling time and maximum error are minimal. The areas of minimum for the four variables are shown in Figure 15. As it can be seen from this figure, a common region exists, where all the four parameters have minimum values. It is extended between 0.04 and 0.08 as to k_d and 1.5 and 2.1 as to M_s. In general as M_s increases, k_d is reduced to be the parameters minimal.

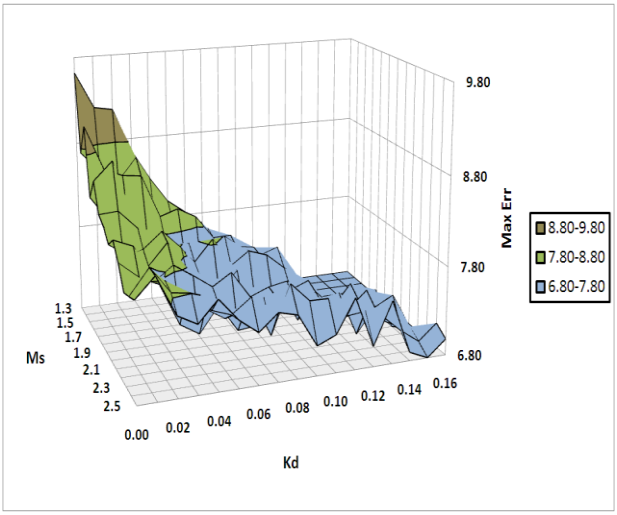

Figure 14. Load disturbance. Maximum error as function of k_d, M_s.

The implementation of these initial simplified simulations offers a picture of the PID sets that could lead to a minimum standard deviation of the modules in RM outlet.

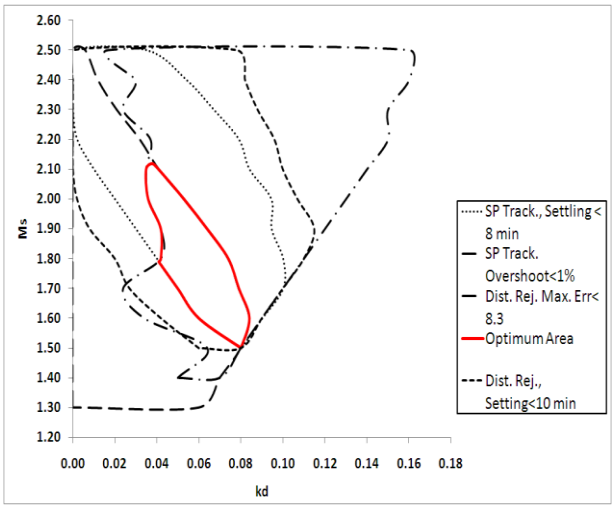

Figure 15. Regions of minimum settling time, overshoot and maximum error.

4.2 Implementation of the Process Simulation in Full Range

The application of the simplified simulations provided an initial approach to the optimization problem. It is expected that the implementation of the complete simulation not only will provide the optimum PID parameters but a further study of the system's parameters can be achieved as well.

Table 3. Simulation data

Total RM Run Time (h)	100	
Constant Composition	Limestone	Clay
Min. Time (h)	4	4
Max. Time (h)	16	16
Period of Constant RM Dynamics		
Min. Time (h)	8	
Max. Time (h)	20	
Sampling Measurement Delay Time (min)	20	
Volume Ratios	Average	Std. Dev
Lim. / Clay	0.5	0.1
Baux./ Iron	3.0	
RM LSF Dynamics		
T_0 (h)	0.19	0.15
t_d (h)	0.41	0.13
RM SM Dynamics		
T_0 (h)	0.33	0.18
t_d (h)	0.33	0.18
Sampling Period (h)	1.0	
LSF Target	97.6	
SM Target	2.5	
Sample Preparation and XRF Reproducibility		
LSF	0.69	
SM	0.018	

Table 3. Cont.		
Initial Feeding Feeders' Settings		
Limestone	0.5	
Iron	0.02	
Mill Dry Production	145	
Electro-filter Flow Rate	8	
Kiln Feed Flow Rate	125	
Filter Oxides	Average	Std. Dev
SiO_2	9.87	0.49
Al_2O_3	4.05	0.14
Fe_2O_3	2.25	0.09
CaO	43.63	0.15
Homo Active Quantity (tn)	428	92
Stock Time Const. $=16.3\cdot Empt\_Met^{-0.602} \pm 1.3$ h		
Initial Homo and Stock Compositions		
SiO_2	13.92	
Al_2O_3	3.34	
Fe_2O_3	2.23	
CaO	42.58	
Stock Silo tn/m	330	
	Min.	Max.
Start up empty meters	4.0	6.0
Empty to Stop RM (m)	3	
Empty to Start RM (m)	5	

A basic data set used in the simulation appears in Table 3. These data are combined with the raw materials analysis shown in Table 2 and with the full set of PID parameters demonstrated in Figures 4 to 7. For these settings the simulator performs 300 runs and the partial results are averaged. Due to the large uncertainty and to have a better approximation of the mean value the 300 runs are iterated three times. Then the three mean values are averaged once more.

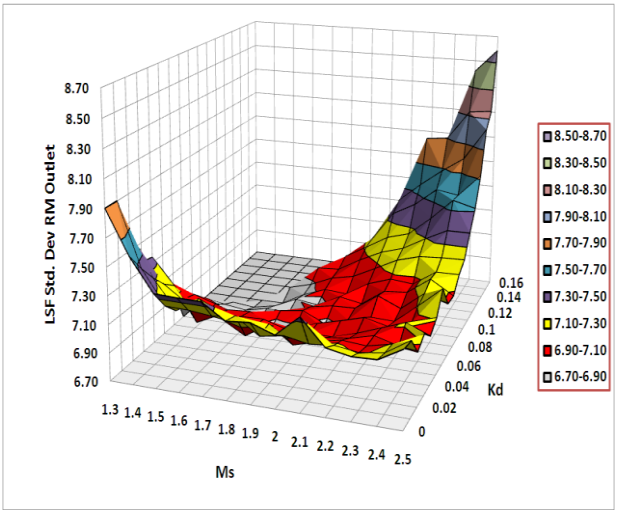

Figure 16. LSF standard deviation in RM outlet

For all the (k_p, k_i, k_d) vectors LSF and SM targets are reached in average, but the modules variance differs considerably. The LSF standard deviations in RM outlet as function of M_s and k_d are shown in Figure 16. A constant PID for SM is operating, not necessarily optimum with $(k_p, k_i, k_d)^T=(0.93, 1.149, 0.4)^T$ corresponding to an $M_s=1.5$.

The results indicate a narrow range of minimum standard deviation extended in the M_s interval [1.4,1.8] and $k_d \geq 0.07$. The percentage of Number of Cuts the LSF_T during the RM operation is shown in Figure 17. From this Figure it can be easily observed that as M_s and k_d are increasing, the number of cuts augments. It can be concluded that a slow controller of small M_s, derives low number of cuts and high variance. On the other hand a fast controller, despite the high number of cuts, produces also a high variance. Between these two limits the optimum parameters area is located. The LSF in the homo silo outlet as function of M_s and k_d appears in Figure 18. The minimum standard deviations of LSF are moved to higher values of M_s and k_d. As to LSF variance in the kiln feed, similar results are obtained. The reason seems to be the high number of cuts as the controller becomes faster. The material's layers in homo and stock silos become thinner and their mixing is better. It shall be reminded that the results are based on the assumption of first order transfer function of each silo. This issue needs further investigation because the time constants of the silos suffer from high uncertainty.

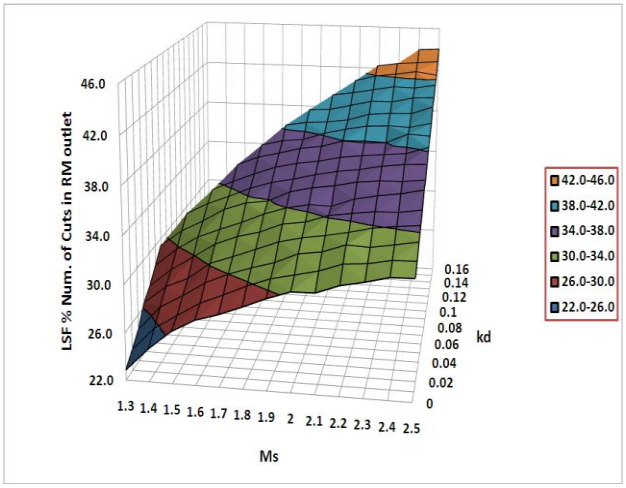

Figure 17. LSF % Number of Cuts the LSF target in RM outlet

The SM standard deviation as function of M_s and k_d is depicted in Figures 19 and 20. As in the previous case, the minimum standard deviation of SM in RM outlet appears in a relatively narrow

region of PID controllers. The optimum area in homo outlet is moved to higher values of M_s and k_d.

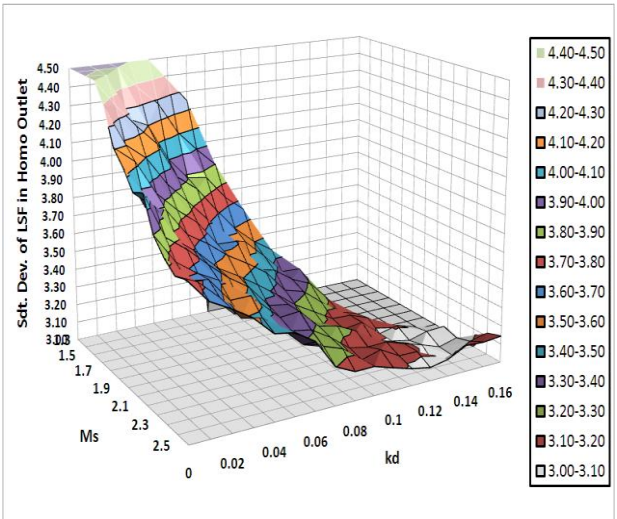

Figure 18. LSF standard deviation in homo outlet

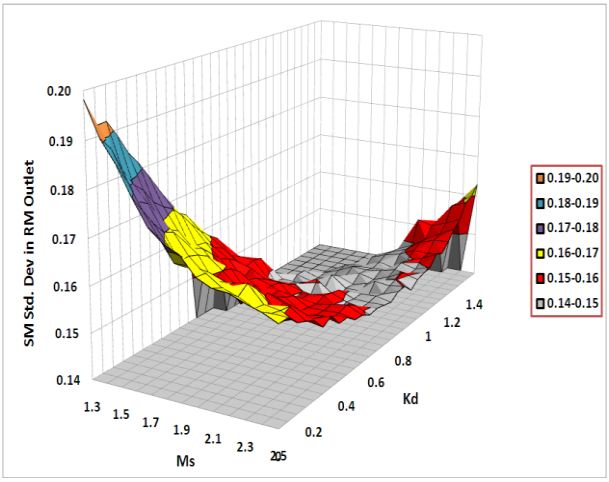

Figure 19. SM standard deviation in RM outlet

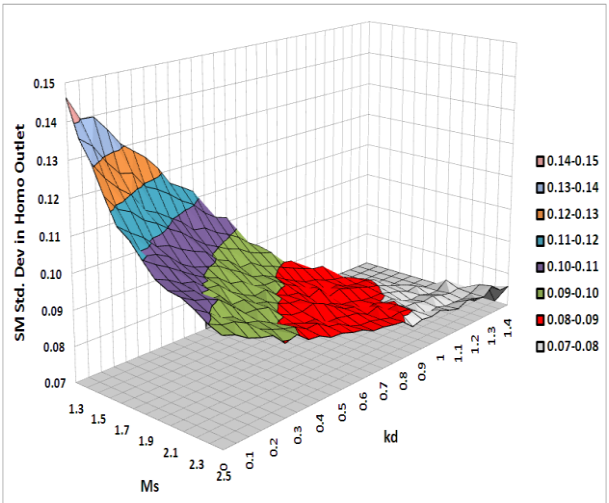

Figure 20. SM standard deviation in homo outlet

4.3 Impact of the Dynamics' Gains on the Optimum PID Parameters

As analyzed in section 2.4 of [5], the implementation of mix design to compute the composition of the raw meal leads to the calculation of the the static gains between inputs and outputs, i.e. for 1% increase of each compound the increase or decrease of the modules is found. The raw materials average analysis shown in Table 2 is utilized. The gain from the limestone feeder to LSF is found equal to 2.64 while the respective gain from additives feeder to SM is 0.388. Even if these gains are found inside the confidence interval of the gains presented in Table 1 apparently they differ from the average values. Possible reasons of this difference are the following:

(a) The dynamical parameters are determined from the data sets presenting a regression coefficient $R \geq 0.7$. In this way all range of the raw materials analysis possibly is not detected.

(b) Due to the sampling plan of the raw materials, probably the computed average analysis does not correspond to the real one during the mentioned period. For this reason a confidence interval is always necessary.

(c) Probable feeders' errors or model mismatches.

To investigate the impact of the dynamics gain on the optimum PID sets providing the minimum variance in RM outlet, the next procedure is followed:

(1) The LSF controller is considered as well as the PID sets shown in Figures 4, 5, found by applying the MIGO method to the dynamical data of Table 1.

(2) The confidence intervals of the clay average analysis are determined.

(3) By adding selected multiples of confidence intervals to the average values of SiO_2, Al_2O_3 and Fe_2O_3 and by subtracting them from the mean value of CaO, new clay analysis are computed of lower LSF.

(4) By implementing the mix design described in [5], the gains between limestone feeder and LSF are found for the all the clays computed in step (3). The results are shown in Table 4.

Table 4. Clay's analysis

SiO_2	43.32	45.12	46.92	48.71	50.06
Al_2O_3	7.52	7.92	8.33	8.73	9.04
Fe_2O_3	3.98	4.17	4.96	4.55	4.70
CaO	20.79	19.36	17.33	16.50	15.43
LSF	15.7	14.0	12.4	11.0	10.0
K_g	2.64	2.74	2.86	2.97	3.06

(5) For each analysis the simulation is applied and the range of PID sets providing standard deviation in mill outlet, differing up to 2% of the minimum one is found.
(6) All these optimum areas are plotted in Figure 21.

From this Figure it is observed that as K_g is increasing, the optimum region generally is moving to lower M_s values. A common optimum area for all the gains appears, extending between 0.054 and 0.09 as to k_d and 1.4 and 1.7 as to M_s. This optimum area is more narrow than the one shown in Figure 15, meaning that the application of the simplified simulations provide an initial picture of the optimum region, while the full simulation offers a restricted region of the optimum location.

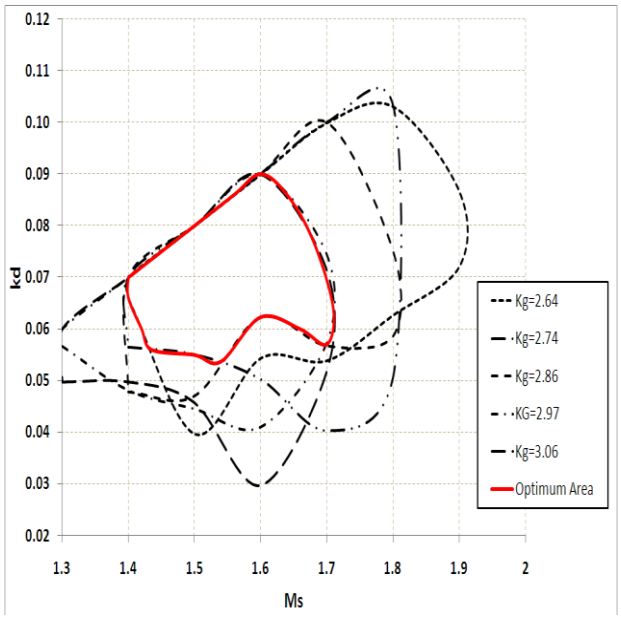

Figure 21. Optimum PID regions for different gains.

For a further investigation of the effect of the dynamics gain on the optimum M_s and the corresponding parameters a second also procedure is applied:

(i) The steps (3) and (4) of the previous procedure are implemented to define clays analysis which produce gains from 2.4 to 3.0 with step of 0.1.
(ii) For each K_g and the time constants presented in Table 1, LSF controllers are parameterized using the MIGO technique for M_s values belonging to the interval [1.3, 1.8].
(iii) The simulator is implemented for each analysis and the corresponding (k_p, k_i, k_d) group. As concerns the other data, the ones shown in Table 2 are utilized.
(iv) For each analysis the PID deriving the minimum variance of LSF in RM outlet is determined as well as the (M_s, k_d) region providing standard deviation up to 2% higher of the optimum one.

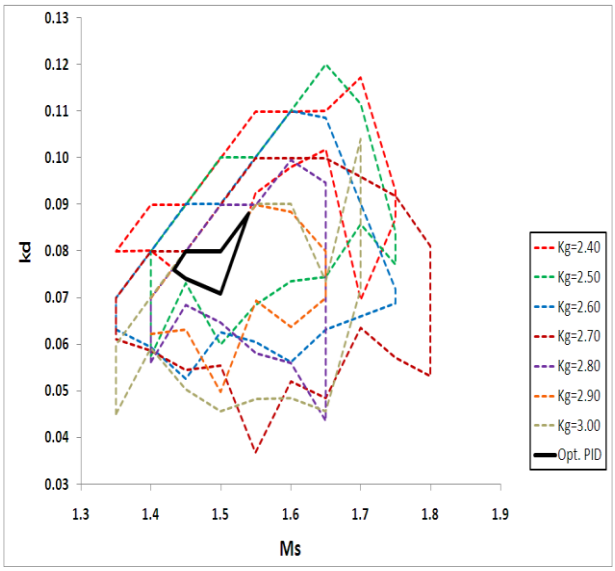

Figure 22. PID optimum area as function of K_g.

The optimum (M_s, k_d) area according to step (iv) is depicted in Figure 22. For all the controllers tested, tuned in accordance with the raw materials analysis, there is a common optimum area located in the M_s interval [1.43, 1.54]. The respective k_d minimum and maximum limits are 0.07 and 0.09 correspondingly. Consequently a PID controller with (M_s, k_d) equal to (1.5, 0.08) belongs always to the optimum area. Apparently the above is valid for the given actual process and materials, with the existing uncertainties. Concerning the SM controller similar results shall be expected. This noteworthy conclusion could provide serious support to the construction of a Model Based Control scheme, combined with a PID controller tuned with the MIGO technique.

5 Conclusions

Based on a dynamical model of the raw materials blending in a closed circuit ball mill an analytical simulation of this grinding installation is developed. The mill dynamics is thoroughly analyzed in [4]. Not only the mill but the homo and storage silos operation is simulated as well. The simulator takes into account the actual variance of the raw materials analysis, by supposing time intervals of constant limestone and clay composition determined using a random numbers generator. The uncertainty of the dynamical parameters is also taken into

consideration. The filter dust and the chemical analysis noise are also incorporated to the simulator.

Two PID controllers are utilized to regulate the LSF and SM modules. The settings of the two independent feeders - limestone and additives - constitute the set of the two control variables. The two controllers tuning is realized by applying the M-constrained integral gain optimization technique to the specific conditions of raw meal production and quality control as described analytically in [5]. For given mill and silos settings the simulator is applied to find the optimum PID sets among those determined by the MIGO technique. As optimization criterion the minimum variance of the two chemical modules in mill outlet and kiln feed is used. The PID sets with maximum sensitivity M_s=1.5 and differential coefficient k_d in the region of its maximum value provide the minimum variance of the two modules under control. Therefore the simulator offers a strong guidance for the selection and implementation of a PID with optimum parameters satisfying simultaneously a robustness constraint and deriving a minimum variance to the process variable.

The development of this kind of simulation provides the possibility to analyze the effect of the process parameters on the raw meal homogeneity, a task which is probably unfeasible to be achieved in real process conditions. Other digital PID implementations, except the one presented here, or other control laws can be investigated as well.

References:

[1] Lee, F.M., The Chemistry of Cement and Concrete,*3rd ed. Chemical Publishing Company, Inc.*, New York, 1971, pp. 164-165, 171-174.

[2] Ozsoy, C. Kural, A. Baykara, C. , Modeling of the raw mixing process in cement industry, *Proceedings of 8th IEEE International Conference on Emerging Technologies and Factory Automation*, 2001, Vol. 1, pp. 475-482.

[3] Kural, A., Özsoy, C., Identification and control of the raw material blending process in cement industry, *International Journal of Adaptive Control and Signal Processing*, Vol. 18, 2004, pp. 427-442.

[4] Tsamatsoulis, D., Modeling of Raw Material Mixing Process in Raw Meal Grinding Installations, *WSEAS Transactions on Systems and Control*, Vol. 5, 2010, pp. 779-791.

[5] Tsamatsoulis, D., Effective Optimization of the Control System for Cement Raw Meal Mixing Process: I. PID Tuning Based on Loop Shaping, *WSEAS Transactions on Systems and Control*, under publication.

[6] Emami, T., Watkins, J.M., Robust Performance Characterization of PID Controllers in the Frequency Domain, *WSEAS Transactions on Systems and Control*, Vol. 4, 2009, pp. 232-242.

[7] Tsamatsoulis, D., Dynamic Behavior of Closed Grinding Systems and Effective PID Parameterization, *WSEAS Transactions on Systems and Control*, Vol. 4, 2009, pp. 581-602.

[8] Keviczky, L., Hetthéssy, J., Hilger, M. and Kolostori, J., Self-tuning adaptive control of cement raw material blending, *Automatica*, Vol. 14, 1978, pp.525-532.

[9] Banyasz, C. Keviczky, L. Vajk, I. A novel adaptive control system for raw material blending process, *Control Systems Magazine*, Vol. 23, 2003, pp. 87-96.

[10] Astrom, K., Hagglund, T., Advanced PID Control, *Research Triangle Park: Instrumentation, Systems and Automatic Society*, 2006.

[11] Ender, D., Process Control Performance: Not as good as you think, *Control Engineering*, Vol. 40, 1993, pp.180-190

[12] Tsamatsoulis, D., Development and Application of a Cement Raw Meal Controller, *Ind. Eng. Chem. Res.*, Vol. 44, 2005, pp. 7164-7174.

[13] Zolotas, A.C., Halikias, G.D., Optimal Design of PID Controllers Using the QFT Method, IEE Proc. – Control Theory Appl., Vol. 146, 1999, pp. 585-590

[14] Gorinevsky, D., Loop-shaping for Iterative Control of Batch Processes, *IEEE Control Systems Magazine*, Vol. 22, 2002, pp. 55—65.

[15] McFarlane, D., Glover, K., A loop shaping design procedure using H_∞ synthesis, *IEEE Transactions on Automatic Control*, Vol. 37, 1992, pp. 759–769.

[16] Lu, G., Ho, D., On robust H_∞ control for non-linear uncertain systems, *Communications in Information and Systems*, Vol. 2, 2002, pp.255-264.

[17] Kim, J.H., Oh, D.C., Robust and Non-fragile H_∞ Control for Descriptor Systems with Parameter Uncertainties and Time Delay, *International Journal of Control*, Automation, and Systems, Vol. 5, 2007, pp. 8-14.

[18] Panagopoulos, H. Astrom, K.J., Hagglund, T., Design of PID controllers based on constrained optimization, *IEE Proceedings-Control Theory and Applications*, Vol. 149, 2002, pp. 32–40.

[19] Astrom, K.J., Hagglund, T., Revisiting the Ziegler–Nichols step response method for PID control, *Journal of Process Control*, Vol. 14, 2004, pp. 635–650.